CrossMark

ORIGINAL ARTICLE

Synthesis, Spectral Characterization, Thermal and Optical Studies of Novel Complexes: 4-(Dimethylamino)benzylidene-4-acetamideaniline and 4-(Dimethylamino)benzylidene-4-nitroaniline

Umesh Neupane[1] · R. N. Rai[1]

Abstract The phase diagram representing solid–liquid equilibrium of entire range of composition and thermodynamic studies of two binary organic systems of 4-dimethylaminobenzaldehyde (DMAB) with two NLO active compounds, p-aminoacetanilide (PAA) and p-nitroaniline (PNA), have been studied by solid state synthetic route. Both systems are independently forming a new entity called intermolecular complex (IMC) and two eutectics on either side of intermolecular complexes. The various thermodynamic parameters such as heat of mixing, entropy of fusion, roughness parameter, interfacial energy and excess thermodynamic functions of IMCs and eutectics were calculated using the heat of fusion values. The TGA and DTA studies were performed to understand the physico-chemical, thermal behavior and unique identity of newly synthesized organic complexes, 4-(dimethylamino)benzylidene-4-acetamideaniline (DMABPAA) and 4-(dimethylamino)benzylidene-4-nitroaniline (DMABPNA), and their respective enthalpy of fusion values were found to be 30.01 and 37.26 kJ mol^{-1}. The higher melting point of both the novel complexes than their parent's compounds reveal the strong molecular interaction between parent components to yield the complex. The FTIR spectral analysis predicts the disappearance of aldehyde peaks of DMAB and NH_2 peaks of PAA and PNA while the appearance of entirely new peaks than that of parent's compounds are the supportive for the formation of new molecular entities. These findings are further supported by FTNMR spectrum studies by observation of disappearance of proton peak of aldehyde of DMAB and amine peaks of PAA and PNA rather formation of new imine proton peak or peaks were observed. The appearance of new peaks in Powder XRD of complexes than those of parent components is further indicative for the formation of complexes. The absorption spectrum of DMABPAA and DMABPNA showed intra-molecular charge-transfer (ICT) excited state absorption at 258 and 241 nm, respectively. Both the IMCs, DMABPAA and DMABPNA, show strong fluorescence with quantum yield 0.66 and 0.93, respectively, in methanol solution.

Introduction

Solid-state chemistry is a fast-developing science and has enhanced by its numerous applications in the high-technology industries [1]. During the last few decades, the synthesis of novel organic materials and study of phase diagram, solidification behavior, atomic packing, optical and nonlinear properties of binary organic systems have been found to be interesting [2–7] to develop the novel materials of specific nature. Due to low transformation temperature, ease in purification, transparency, minimized convection effect and wider choices of materials, the organic materials including eutectics and molecular complexes have gained much importance [8–12] to that of inorganic materials. In order to design the novel materials with 100% yield and to optimize the crystallization processes and crystal growth, the knowledge

✉ R. N. Rai
rn_rai@yahoo.co.in

1 Department of Chemistry, Institute of Science, Banaras Hindu University, Varanasi 221005, India

Springer

of phase diagram study and solid–liquid equilibrium is necessary. The studies are also important for refrigeration and pipeline design, where undesired crystallization can lead to safety risks, [13] and also for separation and purification of organic materials in petrochemical, biological and pharmaceuticals industries [14].

The formation of novel intermolecular compound of entirely new behavior, by exploiting the molecular interaction between two organic compounds having donor (D) and acceptor (A) groups, are of prime importance in continuation of search of new materials. The synthesis of molecular complex has opened the option of engineering the novel molecules by selecting the suitable parent molecules. Furthermore a promising molecule could be synthesized utilizing the option of changing the strength of D and A groups, attached with parent components, as well as by changing their position as changing the strength and position of D and A groups influence the extent and direction of electron transfer between D and A. The separation and distribution of charges, which differs in the excited state to that of the ground state of the complex [15, 16], play a crucial role in producing the specific properties. The complex molecules are useful for the study of solvation dynamics [17], nonlinear optical properties [18] and laser applications [19] as well as for fluorescence probes [20, 21].

In the present investigation, the charge transfer phenomenon due to interactions between aromatic electron acceptor, oxygen, and electron donor, nitrogen, have studied in view of their important role in the field of drug receptor binding mechanism [22, 23] and in developing the novel materials. We have chosen 4-dimethylaminobenzaldehyde (DMAB), which is an important intermediate of dyes and medicine. DMAB belongs to monoclinic crystal system and the centrosymmetric space group *P21/n* [24]. The other two chosen parents are p-aminoacetanilide (PAA) and p-nitroaniline (PNA) having electron donor and electron acceptor moieties with an aromatic ring and known for solvatochromism [25] and large NLO [26] properties. Furthermore, the materials with acetanilide belong to the class of compounds possessing pain-relieving activity [27]. The compounds having acetanilide groups are also have potential relevance to the energy transport in biological systems [28]. Both PAA and PNA belong to orthorhombic crystal system but different space group *Pcab* [29] and P2$_1$2$_1$2$_1$ [30], respectively. The aim of the proposed research work is to synthesize the novel intermolecular complexes by considering the mentioned parent compounds known for their various applications and adopting the solid state synthesis which is solvent free synthesis. The establishing the phase diagram helps to produce the new compound with 100% yield. Further the study has been extended for the characterization of these new complexes for their novelty, optical and thermal behavior. The novelty that we report in this paper is the synthesis of two new

compounds with comparative higher fluorescence property to that of their parent compounds.

Materials and Purification

The parent compounds, 4-dimethylaminobenzaldehyde (DMAB), p-aminoacetanilide (PAA) and p-nitroaniline (PNA), were collected from Aldrich, Germany. These compounds were purified and the purity of each compound was accessed by assessing their melting points and comparing with their literature values. The melting points of DMAB, PAA and PNA were found to be 75.0, 164.0 and 148.0 °C, respectively which are in agreement with their reported values [31].

Phase Diagram

The phase diagram of DMAB-PAA and DMAB-PNA systems were established by the thaw-melt method in the form of temperature–composition curve. In this method [32] the mixtures of two components in different compositions covering the entire range were taken in different test tubes and these test tubes were sealed. The mixture of each test tube was homogenized by repeating the process of melting and mixing followed by chilling in ice cooled water for 4 times. The well homogenized and solidified mixtures of each composition were taken out separately and crushed to fine powders using a pestle and mortar. Toshniwal melting point apparatus, attached with a thermometer which could read up to ± 0.5 °C, has been used to determine the temperature solid–liquid phase transition of different compositions. Finally the phase diagrams were established between mole fraction composition of parent compound on X-axis and their corresponding melting temperature on Y-axis.

Thermal Studies

The enthalpy of fusion of parent compounds, their eutectics and intermolecular complexes were determined by a Differential Scannig Calorimetry (Mettler DSC-4000 system). Indium and zinc samples were used to calibrate the DSC unit. The 4 − 7 mg samples was taken in sealed aluminum pans with a pinhole in the lid and it was heated by the heating rate of 10 °C/min and the same condition was adopted for each samples. The changes in physico-chemical and thermal properties of both intermolecular complex, as a function of temperature was studied by differential thermal analysis (DTA) and thermogravimetric analysis (TGA) using PerkinElmer STA 6000. The samples were heated from 30 to 600 °C at the heating rate of 10 °C min^{-1} under the flow of Nitrogen gas with a flow rate of 20 mL min^{-1} while recording the thermogravimetric curves.

Spectroscopic Studies

The spectral studies, FTIR and NMR, of intermolecular complex and their parent compounds were carried out to understand the structural changes of IMC to that of their parent. The FTIR spectra were recorded in the region 4000–400 cm^{-1} at 300 K, by dispersing them in KBr, using a Perkin Elmer Spectrum 1000 FT-IR Spectrophotometer. NMR spectra of ^{1}H and ^{13}C were recorded in deuterated chloroform at 300 K using JNM-ECZ500R/S1 500 Mhz Spectrometer.

X-ray Diffraction

The X-ray diffraction technique is used for the study of novelty of IMCs and their crystallinity. The powder X-ray diffraction (XRD) patterns of pure compounds, eutectics and IMCs were recorded using an 18 kW rotating (Cu) anode based Rigaku powder diffractometer fitted with a graphite monochromator in the diffracted beam. The samples were scanned from 10 to 70° with a scanning rate of 4°/min.

Optical Characterization

The absorption spectra of the intermolecular complex compounds along with their parent components were studied in the solution of MeOH solvent maintaining 1 ppm concentration using UV/Vis/NIR (JASCO model V-670) spectrometer from 190 to 1200 nm at 300 K. The Fluorescence spectra were also recorded using Varian Cary Eclipse Fluorescence Spectrophotometer at 300 K using the same solutions.

Result and Discussion

Phase Diagram Study

The Phase diagram of 4-dimethylaminobenzaldehyde (DMAB)–p-aminoacetanilide (PAA) and DMAB-p-nitroaniline (PNA) systems, constructed in terms of temperature-composition curve, showed the formation of DMABPAA and DMABPNA intermolecular complexes, respectively. In each case, the IMCs are formed at equimolar composition. The IMCs are surrounded by two eutectics as shown in Fig. 1a, b. The slight increase in mole fraction of DMAB, decreases the melting point of PAA and PNA and it go on decreasing, with increase of DMAB, till it attend the lowest melting point called E_1 in both systems. The respective mole fraction of DMAB for eutectic E_1 in DMAB-PAA and DMAB-PNA systems were 0.14 and 0.18 and their corresponding melting temperature were 156.0 and 135.0 °C. Further, addition of DMAB causes continuous increase in the melting point of binary mixture up to the equimolar

composition where it attained a maximum temperature 218.0 °C for DMAB-PAA and 202.0 °C for DMAB-PNA systems. These maximum temperatures are the congruent melting temperatures where the compositions of liquid and solid phase are identical. Beyond this composition, the melting temperatures of binary mixtures go on decreasing up to the second eutectic point E_2 where it acquires a minimum temperature of 74.0 °C at 0.98 mol fraction of DMAB in case of DMAB-PAA system and 72.0 °C at 0.95 mol fraction of DMAB in DMAB-PNA system. For each eutectic, the intermolecular complex behaves as one of the parent components. The finding of higher melting temperature than their parent components, in both the systems, suggest the formation of new and stable entity which would be stronger than the parent components [33]. At eutectic temperature, a liquid phase is in equilibrium with two solid phases and the eutectic reaction may be schematically represented as:

$$L \leftrightharpoons S_1 + S_2 \tag{1}$$

Similarly at maximum melting temperature, the composition of intermolecular complex is in equilibrium with their solid and liquid phases which may be represented as:

$$A + B \leftrightharpoons AB_{(Liquid)} \rightarrow AB_{(Solid)} \tag{2}$$
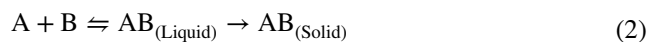
The phase diagram studies of both systems revealed that there are three invariant points, eutectic-1, intermolecular compound and eutectic-2 in each systems. The melting point of selected compositions covering entire range of DMAB-PAA and DMAB-PNA systems are tabulated in supplementary Table S1 and S2. The schemes for the synthesis of both the intermolecular complexes, DMABPAA and DMABPNA, are given in supplementary figure S1 and S2, respectively.

Thermochemistry

Thermal properties of parent components, eutectics and intermolecular complexes of both the systems were studied in order to explain the thermodynamic feasibility of the system. Thermodynamic parameters like enthalpy of fusion, entropy of fusion, roughness parameter, interfacial energy, grain boundary energy and excess functions were studied.

Enthalpy of Fusion

The idea about the nature of interaction between the two components forming the eutectics and complex compound could be obtained from their enthalpy of fusion value. The studies of thermal behavior with temperature and the plots for pure components, the eutectics and the intermolecular compound of both systems are given in Fig. 2a, b. The experimentally obtained values of enthalpy of fusion and the computed values using the mixture law are given

Fig. 1 **a**) Phase diagram of DMAB–PAA system. **b**) Phase diagram of DMAB–PNA system
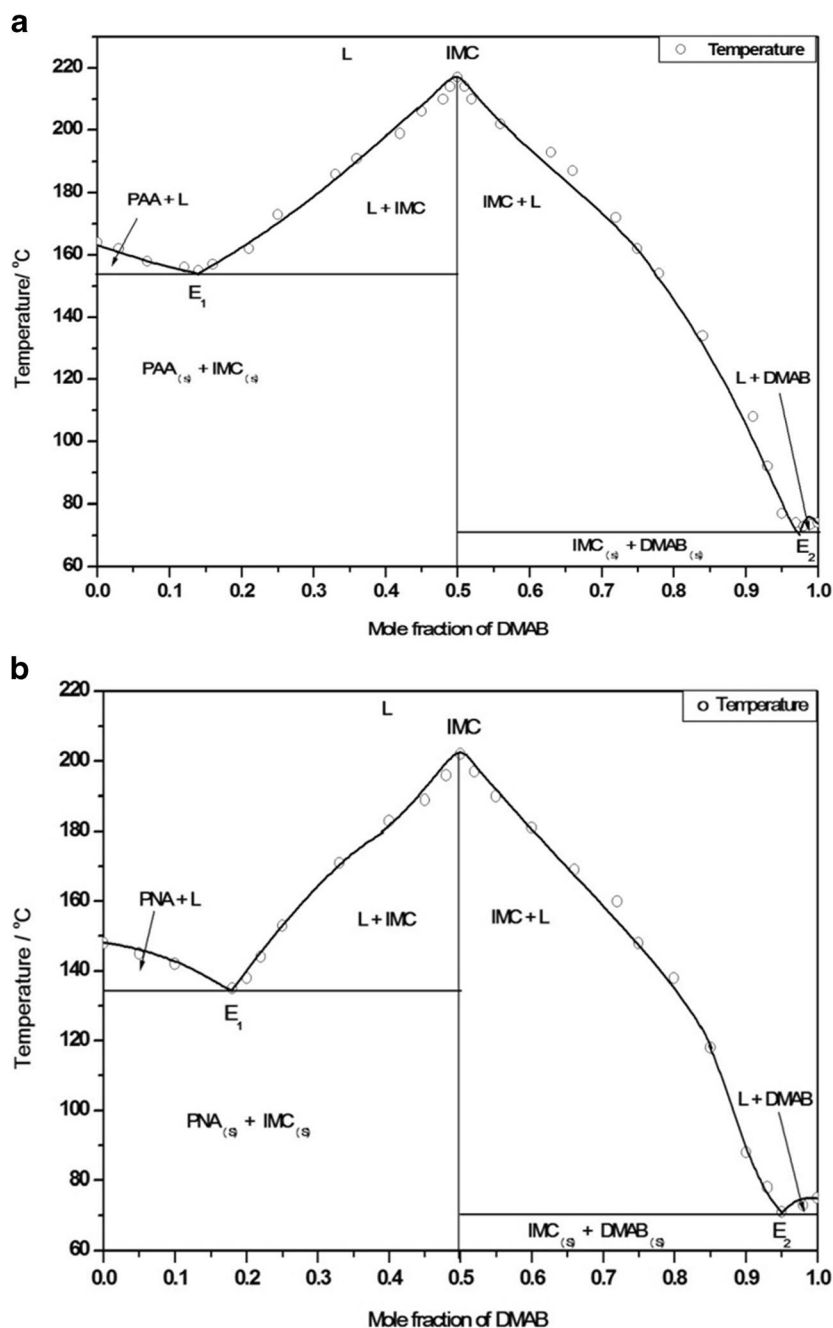
in Table 1. The values of enthalpy of mixing ($\Delta mixH$), obtained by substracting calculated values of enthalpy of fusion from experimentally determined values, predict the particular association of molecules in binary eutectics and intermolecular complex. Based on association, three types of structures are suggested [33]: quasi-eutectic for $\Delta_{mix}H > 0$, clustering of molecules for $\Delta_{mix}H < 0$ and molecular solution for $\Delta_{mix}H = 0$. The enthalpies of mixing for both eutectics of DMAB-PAA system and eutectic-2 of DMAB-PNA were found to be negative which suggest the clustering of molecules in binary melt. On the other hand, positive

value of $\Delta_{mix}H$ for the eutectic-1 in DMAB-PNA system suggests quasi-eutectic structure formation between the molecules in binary melt. The values of $\Delta_{mix}H$ are also tabulated in Table 1. The entropy of fusion $\Delta_{fus}.S$ value of parent compounds, eutectics and intermolecular complex were also calculated and tabulated in Table 1. The $\Delta_{fus}.S$ values are positive for all pure and binary suggest that the process of melting favours. The influencing parameters for crystal growth and crystal's morphology such as interfacial energy (σ), roughness parameter (α) and grain boundary energy (γ) were also calculated for the parent components, eutectics
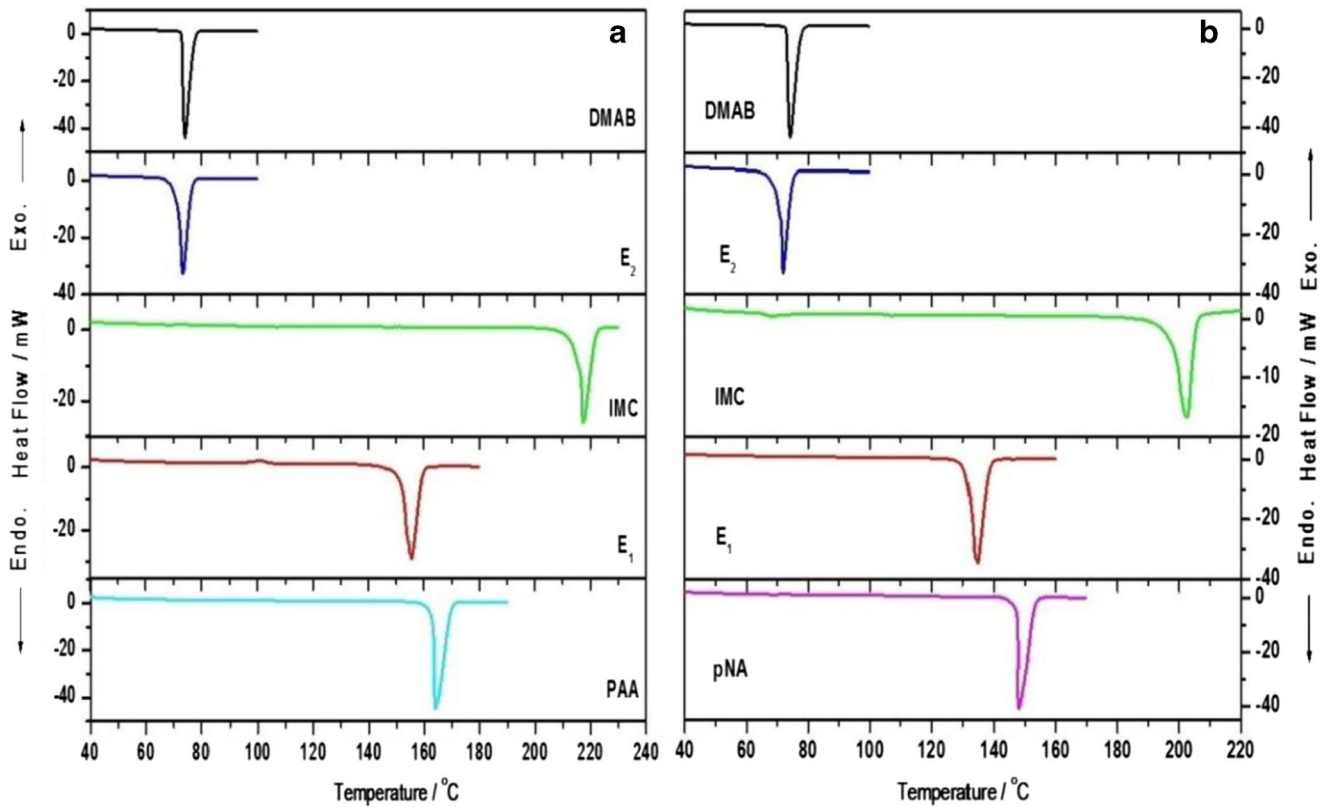
Fig. 2 DSC curves of (**a**) IMC, DMAB, PAA and eutectics (**b**) IMC, DMAB, PNA and eutectics

and the intermolecular compounds using following equations [34]:

$$\sigma = \frac{C.\Delta_{fus}H}{(N_A)^{1/3}(V_m)^{2/3}} \qquad (3)$$

where, N_A is the Avogadro Number, V_m is the molar volume, and parameter C lies between 0.30 and 0.35. The value of C used for calculation was 0.35.

$$\alpha = \xi \, \Delta_{fus}H/RT \qquad (4)$$

where ξ is a crystallographic factor which is generally equal to or less than one, for present calculation it is used $\xi = 1$.

$$\gamma = 2\sigma \cos \theta \qquad (5)$$

where θ is the angle between tangent on interface and is known as grain boundary angle. The determination of exact value of grain boundary energy (γ) is complicated, however the range of γ could be approximated because the value of $\cos\theta$ may be less than or equal to one.

The value of $\alpha > 2$, suggest that the interface is quite smooth and the crystal develops with a faceted morphology. On the other hand if $\alpha < 2$, the interface is rough and many sites are continuously available and the crystal develops with a non-faceted morphology. In the present studies,

the values of α being greater than 2 in both the cases suggest that phases would grow with facetted morphology. The value of σ, α and γ for all components of both systems are given in Table 2.

Excess Thermodynamic Functions

To understand the divergence from ideal behavior of eutectics and nature of interaction between components forming eutectics, the excess thermodynamic functions in terms of excess free energy (g^E), excess enthalpy (h^E) and excess entropy (s^E) were studied [35] by using the following equations:

$$g^E = RT\left[x_1 \ln \gamma_1^1 + x_2 \ln \gamma_2^1\right] \qquad (6)$$

$$h^E = -RT^2\left[x_1 \frac{\partial \ln \gamma_1^1}{\partial T} + x_2 \frac{\partial \ln \gamma_2^1}{\partial T}\right] \qquad (7)$$

$$s^E = -R\left[x_1 \ln \gamma_1^1 + x_2 \ln \gamma_2^1 + x_1 T \frac{\partial \ln \gamma_1^1}{\partial T} + x_2 T \frac{\partial \ln \gamma_2^1}{\partial T}\right] \qquad (8)$$

From Eqs. (6)–(8), it is apparent that the activity coefficient and its variation with temperature are required to

Table 1 Melting temperature, heat of fusion, heat of mixing and entropy of fusion of DMAB-PAA and DMAB-PNA systems

System	Component	Melting Temperature (K)	Heat of fusion (kJ mol^{-1})	Heat of mixing (kJ mol^{-1})	Entropy of fusion (kJ mol^{-1} K^{-1})
DMAB-PAA	DMAB	348.0	20.64		0.059
	PAA	437.0	30.36		0.695
	Eutectic-1				
	Exp	429.0	30.01	−2.28	0.069
	Cal		32.29		
	Eutectic-2				
	Exp	346.0	20.57	−0.74	0.059
	Cal		21.31		
	Intermolecular Complex				
	Exp	491.0	37.26	11.75	0.076
	Cal		25.51		
DMAB-PNA	DMAB	348.0	20.64		0.059
	PNA	421.0	21.48		0.051
	Eutectic-1				
	Exp	408.0	25.14	0.16	0.062
	Cal		24.98		
	Eutectic-2				
	Exp	345.0	19.99	−1.71	0.058
	Cal		21.70		
	Intermolecular Complex				
	Exp	475.0	31.23	10.16	0.066
	Cal		21.06		

Table 2 Roughness parameter, interfacial energy and grain boundary energy of DMAB-PAA system (DMAB, PAA, eutectic-1, eutectic-2 and IMC) and DMAB-PNA system (DMAB, PNA, eutectic-1, eutectic-2 and IMC)

System	Components	Roughness parameter(α)	Interfacial energy (σ) erg.cm^{-2}	Grain boundary energy (γ) erg. cm^{-2}
DMAB-PAA	DMAB	7.13	32.41	64.82
	PAA	8.35	50.37	100.74
	Eutectic-1	8.41	47.85	95.70
	Eutectic-2	7.15	32.77	65.54
	IMC	9.12	41.39	82.78
DMAB-PNA	DMAB	7.13	32.41	64.82
	PNA	6.13	42.09	84.18
	Eutectic-1	7.41	40.34	80.69
	Eutectic-2	6.97	32.35	64.70
	IMC	7.90	31.83	63.66

calculate the mentioned excess function. Activity coefficient (γ_i^l) could be evaluated by using the equation,

$$-\ln\left(x_i\,\gamma_i^l\right) = \frac{\Delta_{\text{fus}}H_i}{R}\left(\frac{1}{T_{\text{fus}}} - \frac{1}{T_i}\right) \quad (9)$$

where x_i, $\Delta_{\text{fus}}H_i$, T_i and T_{fus} are mole fraction, enthalpy of fusion, melting temperature of component i and melting temperature of eutectic, respectively. The variation of

activity coefficient with temperature can be calculated by differentiating Eq. (9) with respect to temperature.

$$\frac{\partial\ln\gamma_1^l}{\partial T} = \frac{\Delta_{\text{fus}}H_i}{RT^2} - \frac{\partial x_i}{x_i\partial T} \quad (10)$$

where, $\partial x_i/\partial T$ in this expression has been evaluated by considering two points on either side of the eutectic.

The positive values of excess free energy of E_1, for both the systems, suggest that the interactions between like molecules (DMAB–DMAB and IMC–IMC) are stronger than that of unlike molecules (DMAB-IMC). On the other hand, negative values of g^E for E_2, in both the systems, indicate association between unlike molecules (IMC-PAA, DMAB-PAA and IMC-PNA DMAB-PNA) are stronger. The values of g^E, h^E and s^E for both eutectics of both the systems are tabulated in Table 3.

TG and DT Analyses of DMABPAA and DMABPNA Complexes

The TG analyses of DMABPAA and DMABPNA complexes have been studied in the temperature range from 30 to 600 °C and have shown in Fig. 3. The TG analysis of DMABPAA complex shows there is no any weight loss up to 260 °C with no any phase transition and material is quite stable up to 260 °C. Beyond the 265 °C temperature sudden weight loss occurs till 420 °C. Further very slow weight loss occurs with temperature and 20% residual mass decomposes after 420 °C. The TGA curve of DMABPNA complex indicates that it is thermally stable with no any phase change up to 210 °C. After that decomposition

process commences and infers the weight loss in steps. The main decomposition step take place at 215 °C and undergoes sharp weight loss (60%) up to 325 °C and after that slow weight loss occur up to 600 °C. The DTA curves of both the systems are shown in supplementary Fig. S2 which also support the sharp melting points of the complexes as observed in DSC studies.

Spectroscopic Studies

FTIR and NMR Analysis of DMAB-PAA System

In the FTIR of DMAB, peaks observed at 2796.09 cm^{-1} is due to H–C$=$O stretching and peak at 2714.56 cm^{-1} is due to C–H stretching of aldehyde group. The absorption peak at 1662.36 cm^{-1} has been assigned to C$=$O stretching. These findings identify the presence of aldehyde group. The other peaks at 1232.46 and 1602.13 cm^{-1} are due to C–N and C–C stretching, respectively. In ^{13}C NMR spectrum of DMAB, aldehyde carbon appears at higher δ (191 ppm) and two methyl carbons at lower δ (40 ppm) values. The chemical shift at 131 and 111 and 151 ppm correspond to the aromatic carbons at o-, m- and p-position carbons relative to the carbon attached

Table 3 Excess thermodynamic functions for the eutectics of DMAB-PAA and DMAB-PNA systems

System	Components	g^E (kJ mol^{-1})	h^E (kJ mol^{-1})	s^E (J mol^{-1} K^{-1})
DMAB-PAA	Eutectic-1	0.3968	16.8634	0.0383
	Eutectic-2	-0.0686	9.5284	0.0277
DMAB-PNA	Eutectic-1	0.2057	-1.6004	-0.0046
	Eutectic-2	-0.0821	13.073	0.0381

Fig. 3 TGA curves of DMABPAA and DMABPNA complexes
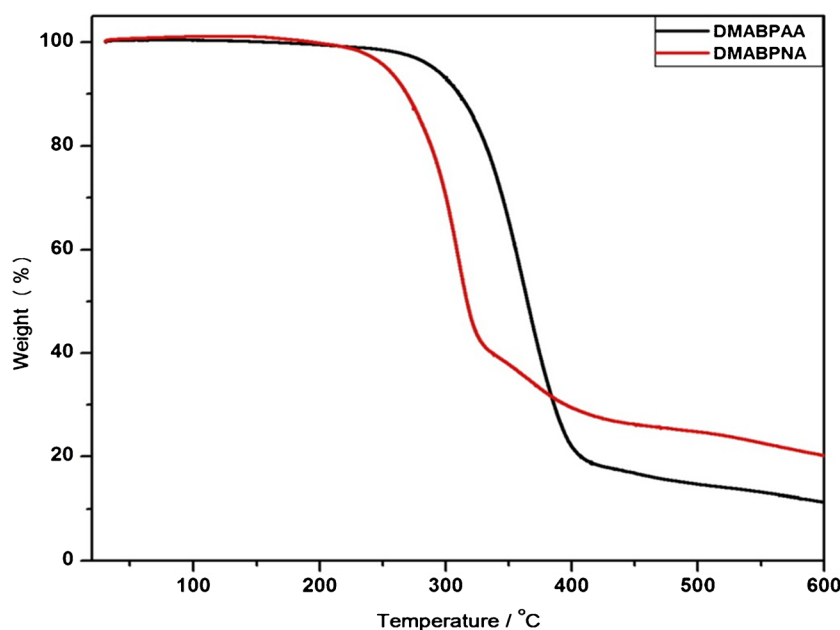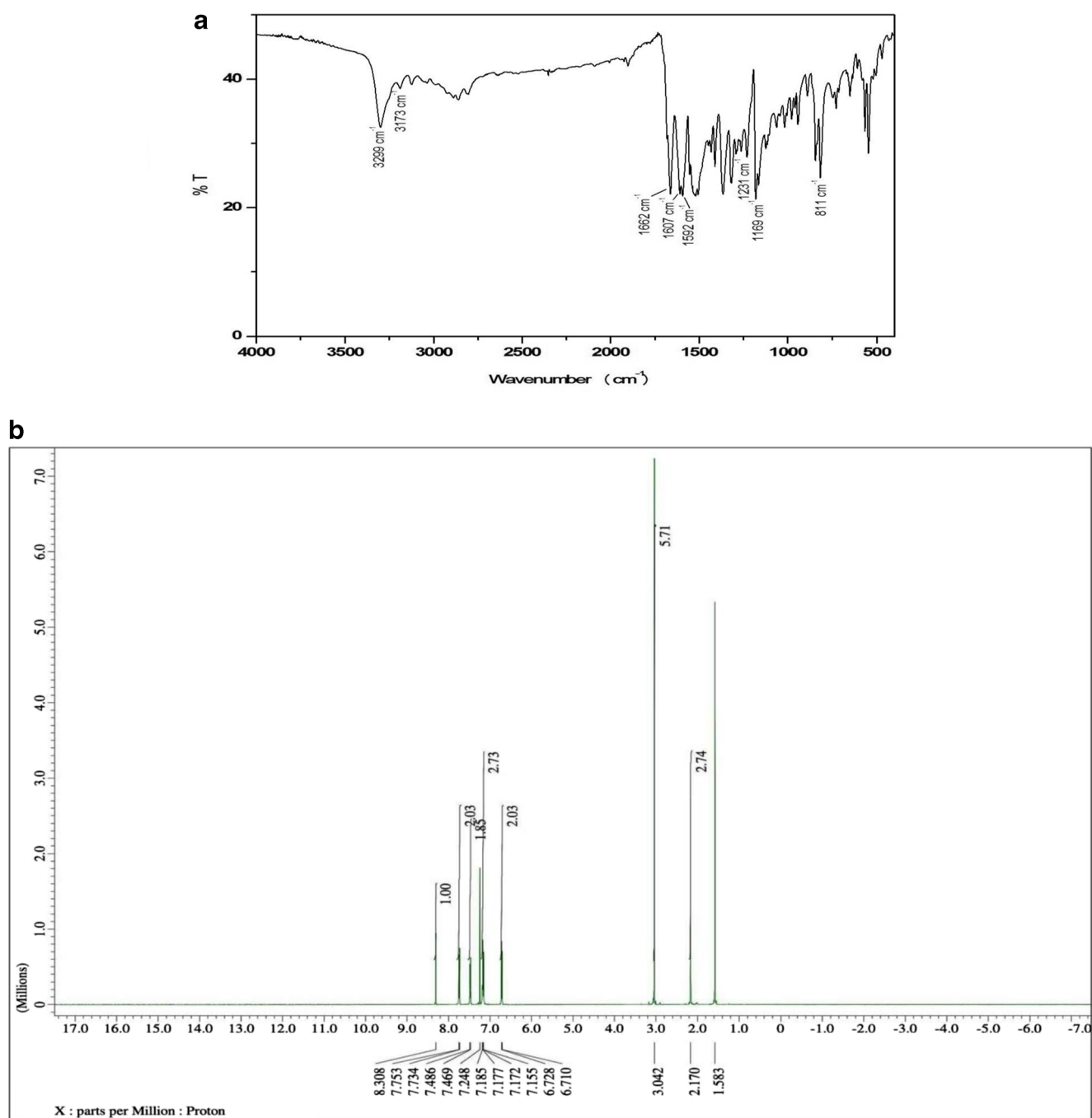
Fig. 4 **a**) FTIR spectrum of DMABPAA complex. **b**) Proton NMR spectrum of DMABPAA. **c**) Carbon NMR spectrum of DMABPAA

with functional aldehyde group which gives its own peak at 127 ppm. In ^{1}H NMR of DMAB, the peaks appear at $\delta = 9.73$ ppm (1H s) is due to aldehydic proton, 7.73 ppm (2H d) and 6.70 ppm (2H d) are due to aromatic proton at ortho and meta position of aldehyde group and intense peak at 3.07 ppm (6H s) is due to two methyl amino group at para position. The FTIR and NMR spectra of DMAB have shown in Fig. S3 and S4 as supplementary information.

In the FTIR spectrum of PAA, the NH$_2$ group is identify due to its six internal modes of vibrations as: peaks observed at 3371.93 and 3244.15 cm^{-1} correspond to asymmetric and symmetric stretching while peaks at 1603.58 and 1089.75 cm^{-1} are the result of scissoring and rocking mode of NH$_2$ group, respectively. The NH$_2$ wagging and C–NH$_2$ in-plane bending mode have appeared at 624.02 and 419.74 cm^{-1}, respectively. In the ^{13}C NMR spectrum of PAA, aromatic carbons appeared
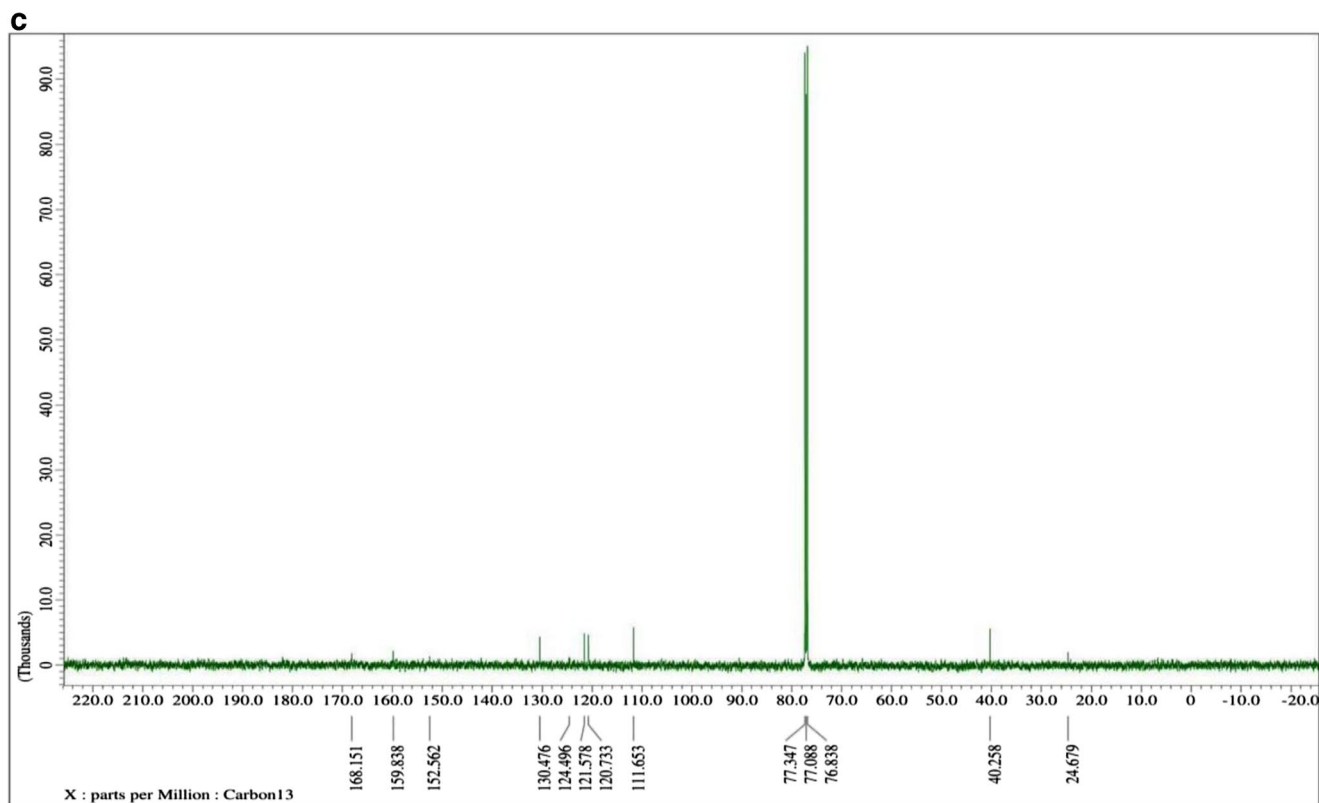
c

Fig. 4 (continued)

at 114 and 121 ppm correspond to o- and m-position carbons with respect to the carbon (142 ppm) which contains amine group. The carbonyl carbon and methyl carbon give their signals at 168 and 23 ppm, respectively. Carbon bonded with acetanilide group appeared at 140 ppm in the spectrum. In proton NMR of PAA, 5 different types of protons are observed at different δ values. The peaks at δ = 8.53 ppm (1H s) is due to amide proton, at 7.27 and 6.62 ppm (2H d) are due to aromatic protons at ortho and meta position of amide group, respectively. The singlet peak at 3.78 and 2.09 ppm are due to amine proton and methyl proton, respectively. The FTIR and NMR spectra of PAA have given in supplementary as Fig. S5 and S6, respectively.

The FTIR spectral analysis of newly synthesized 4-(dimethylamino)benzylidene-4-acetamideaniline (DMA-BPAA) complex is shown in Fig. 4a. The spectrum showed appearance of entirely new peaks and disappearance of peaks those were assigned for NH_2 group of PAA and C=O group of DMAB. A new strong peak at 3299.10 cm^{-1} explaining to C–H stretching absorption of azomethine and a peak obtained at 1592 cm^{-1} confirm the formation of imine bond (C=N) rather than C=N stretching peak of azomethine benzylidene anilines at about 1600 cm^{-1} [36]. In ^{13}C NMR of the complex, the peak assigned for carbonyl carbon

of DMAB (190.0 ppm) was found to be absent rather a new single peak has observed at 159.84 ppm, which could be assigned to azomethine carbon (CH=N). In the proton NMR spectrum of DMABPAA complex, the peak assigned for NH_2 proton of PAA (4.78 ppm) was absent instead of this a new singlet peak observed at 8.3 ppm is due to imine proton (CH=N). The appearance of new peaks and disappearance of some of parents' peaks are confirming the existence of new entity which supports the findings of phase diagram and thermal studies. Proton and carbon NMR spectra of the complex are shown in Fig. 4b, c, respectively.

FTIR and NMR Study of DMAB-PNA System

The FTIR and NMR studies of one of the parent, DMAB, have discussed earlier. In the FTIR spectrum of PNA, the peaks of NH_2 group of PNA exhibit at 3483.28 and 3362.67 cm^{-1} due to asymmetric and symmetric stretching of N-H bond while peaks at 1632.48 and 999.31 cm^{-1} are the result of scissoring and rocking mode of NH_2 group, respectively. Peaks at 632.87 and 490.54 cm^{-1} are the respective peaks due to C–C stretching and C–NH_2 in-plane bending. Asymmetric and symmetric stretching of NO_2 has observed at 1505.70 and 1327.31 cm^{-1}, respectively. The weak signals observed in 3000 to 2200 cm^{-1} region are due
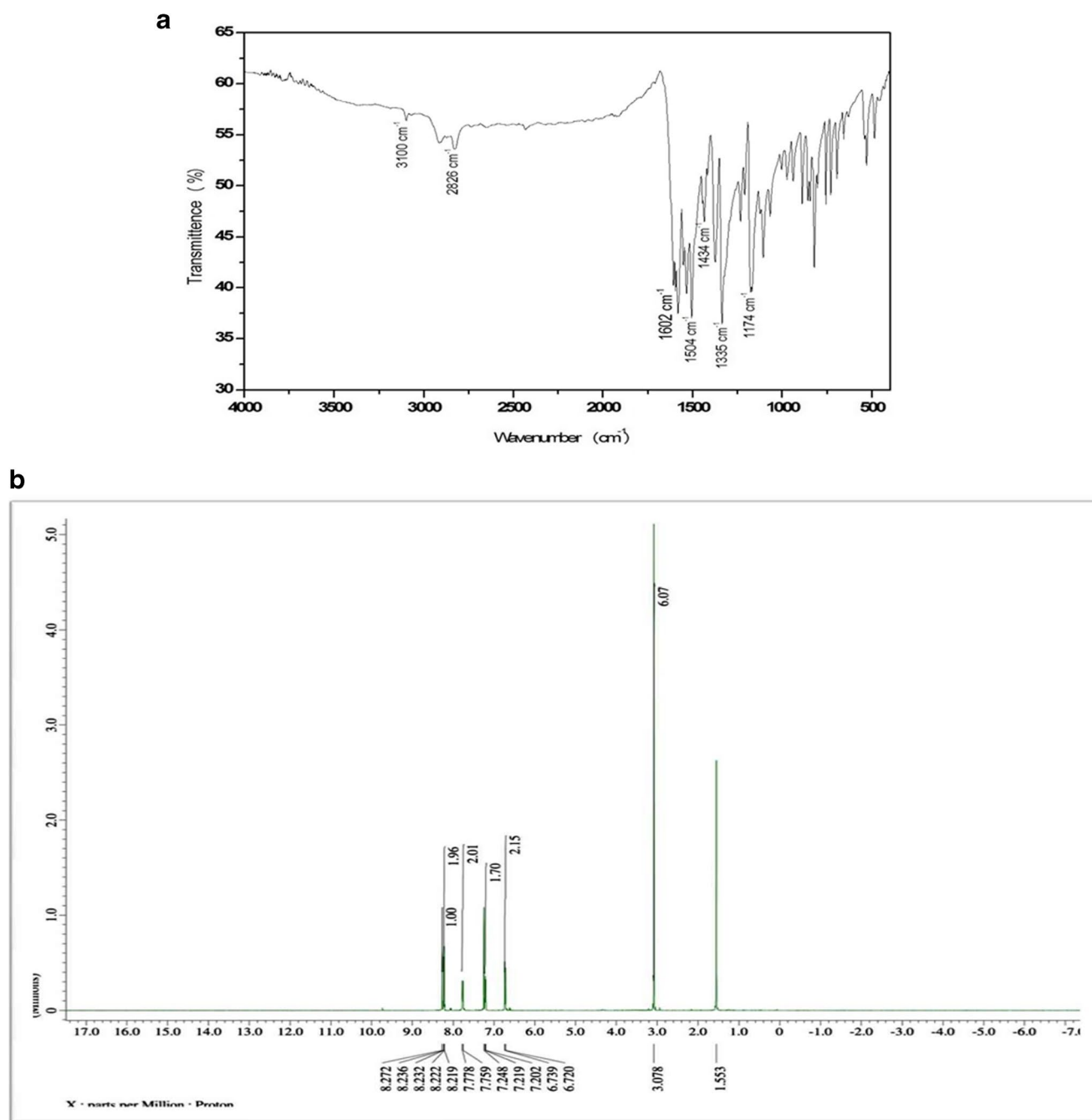
a

b

Fig. 5 **a**) FTIR spectrum of DMABPNA complex. **b**) Proton NMR spectrum of DMABPNA. **c**) Carbon NMR spectrum of DMABPNA

to overtones and combination bands. In proton NMR spectrum, peaks at 8.07 and 6.60 ppm are due to aromatic proton at o- and p-position of nitro group. The amine proton peak has observed at 6.62 ppm. In ^{13}C spectrum, peaks correspond to 152.49 and 139.26 ppm are due to aromatic carbon attached with NH_2 and NO_2 group. The peaks observed at 113.46 and 126.45 ppm correspond to o- and m-position carbons relative to carbon of NH_2 group. The FTIR and NMR

spectra of PNA are given in supplementary Fig. S7 and S8, respectively.

In the FTIR and NMR spectra of intermolecular compound 4-(dimethylamino) benzylidene-4-nitroaniline (DMABPNA), peaks of aldehyde group of DMAB and amino group of PNA have been disappeared instead some new strong peaks have observed in FTIR and NMR. In FTIR, Benzylidene anilines display their C=N stretching vibration at about 1600 cm−1 [36]. Hence the band obtained at
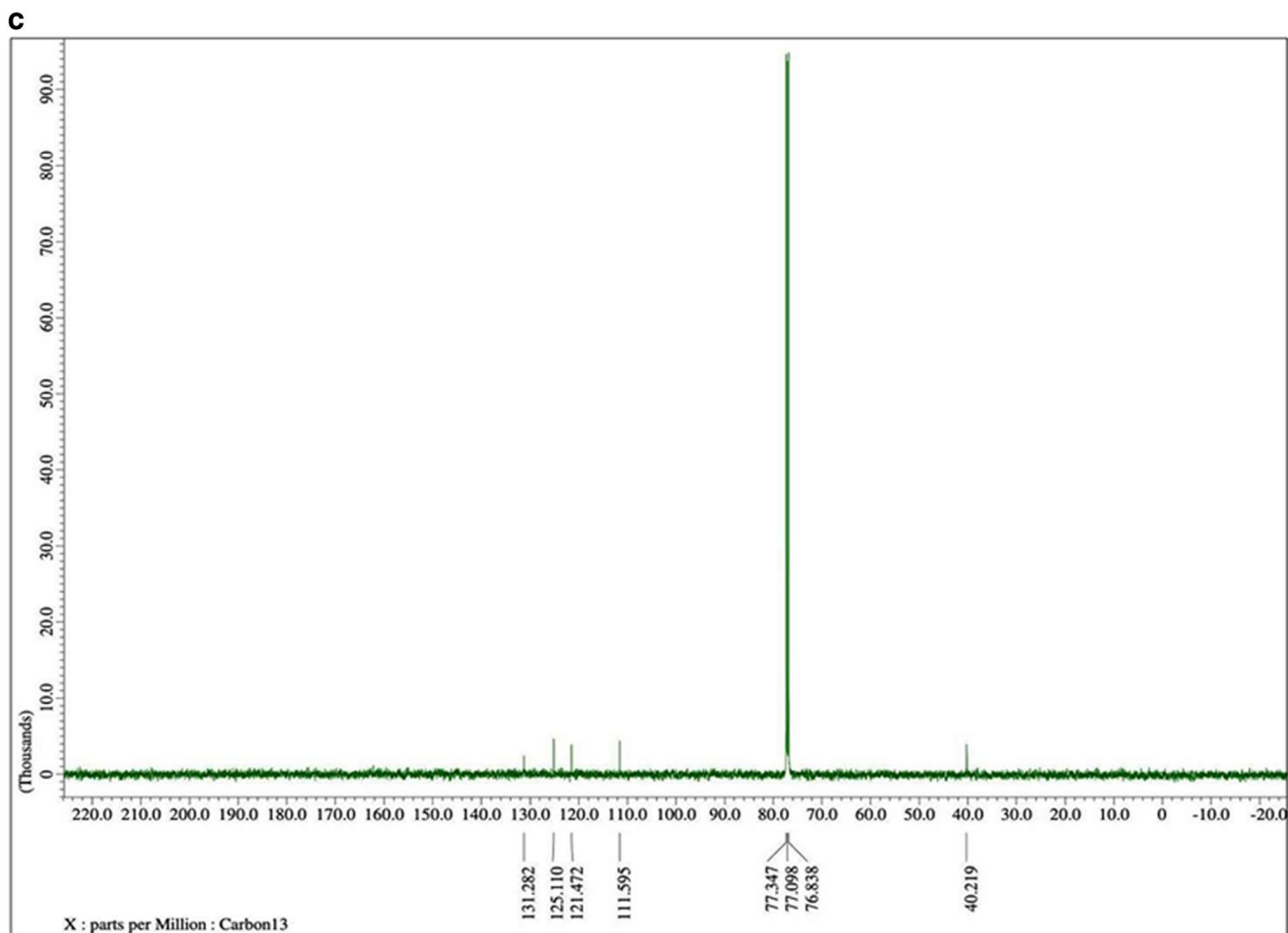
c

Fig. 5 (continued)

1602 cm^{-1} confirms the formation of imine group (C=N) as a result of the condensation reaction between aldehyde and amine while symmetric and asymmetric stretching vibrations of amino and aldehydic groups are completely absent. Peak observed at 3100 cm^{-1} is due to symmetric stretching of CH=N and is shown in Fig. 5a. In ^{1}H NMR spectrum, the singlet new peak appeared at 8.27 ppm is due to imine proton (CH=N). The other peaks at 8.23, 7.77, 7.21 and 6.73 ppm are due to aromatic protons and the strong peak appeared at 3.07 ppm correspond to methyl group. This fact is also supported by ^{13}C spectrum in which peak due to aldehydic carbon at 190 ppm is absent instead a weak signal of azomethine carbon exist at 162 ppm. The Proton and NMR spectra of DMANPNA complex are shown in Fig. 5b, c, respectively.

X-ray Diffraction Studies

Powder X-ray diffraction (PXRD) patterns of parent compounds, their eutectics and intermolecular complex (IMC) of both systems, DMAB-PAA and DMAB-PNA, are depicted in Fig. 6a, b, respectively. It is evident from the figure that the powder XRD patterns of IMC shows the appearance of some new peaks which could not be assigned for either of the parent components. In addition to this, change in the intensities of some of the parent peaks was also observed suggesting thereby the formation of a new compound [37]. In PXRD pattern of DMAB-PAA systems, the E_1 shows some peaks of PAA and DMABPAA while that of E_2 gives the peaks of DMABPAA and DMAB. Similarly, In DMABPNA system, E_1 retains the XRD peaks of PNA and DMABPNA while E_2 retains the peaks of DMABPNA and DMAB. The appearance of peaks of either of parents' components and IMC in E_1 and E_2 indicate that E_1 and E_2 are assumed to be the mechanical mixture of IMC and one of the parent components in both the systems. Appearance of entirely new peaks in DMABPAA and DMABPNA complexes, which could not be assigned for their parent compounds, support the formation of molecular complexes as new entities and the existence of peaks also infer their crystalline nature.

Optical Study

UV–Vis. Absorption of DMABPAA and DMABPNA Complexes

The absorption spectrum of both the complexes, DMAB-PAA and DMABPNA, along with their parent components are shown in Fig. 7a, b, respectively. The absorption spectra of complexes have clearly indicated the changes due to change in molecular structure and functional groups to that of their parent compounds. The lower bands assigned at 258 nm for DMABPAA and 251 nm for DMABPNA are due to transition of electrons of aromatic ring from $\pi\rightarrow\pi^*$ and higher bands at 365 nm for DMABPAA and 346 nm for DMABPNA are attributed to $n\rightarrow\pi^*$ transition due to imine (CH=N) group. The lower absorption band of DMABPAA shows red shift with respect to DMAB in DMAB-PAA system, and in DMAB-PNA system, the complex shows red shift to that of PNA with increased intensity, which might be due to the increase in extent of conjugation in the complexation. But at higher absorption band, the complex DMABPAA is red shifted with respect to DMAB and the complex DMABPNA is blue shifted with respect to PNA. The blue shift can be explained for the greater stability of paired electron in ground state than unpaired electron in excited state

[38]. It is considered that electron density of C=O bond reduced when water molecule is eliminated during complex formation process. It is because of the presence of strong electron withdrawing groups, acetanilide in DMABPAA and nitro in DMABPNA, present in the complex molecules [39, 40] and also π electrons of C=N bridge involve in the resonance stabilization [41].

Emission Spectra of DMABPAA and DMABPNA Complexes

The emission spectra of DMABPAA and DMABPNA complexes along with their parents compounds were recorded by excitation them with their λ_{max} wavelengths. The parent compounds PAA and PNA do not show any noticeable fluorescence upon excitation with their respective λ_{max} excitation. However, DMAB shows emission at 380 nm upon excitation at 340 nm but the emission intensity was found to be very low. The both complexes at their respective λ_{max} excitation in higher wavelength, 365 nm in DMABPAA and 346 nm in DMABPNA, have not shown any significant fluorescence spectra. However, using their lower excitation wavelengths, 258 nm in DMABPAA and 251 nm in DMABPNA, both the complexes have show significant strong fluorescence intensity as shown in Fig. 8a. Noticeably both complexes show a
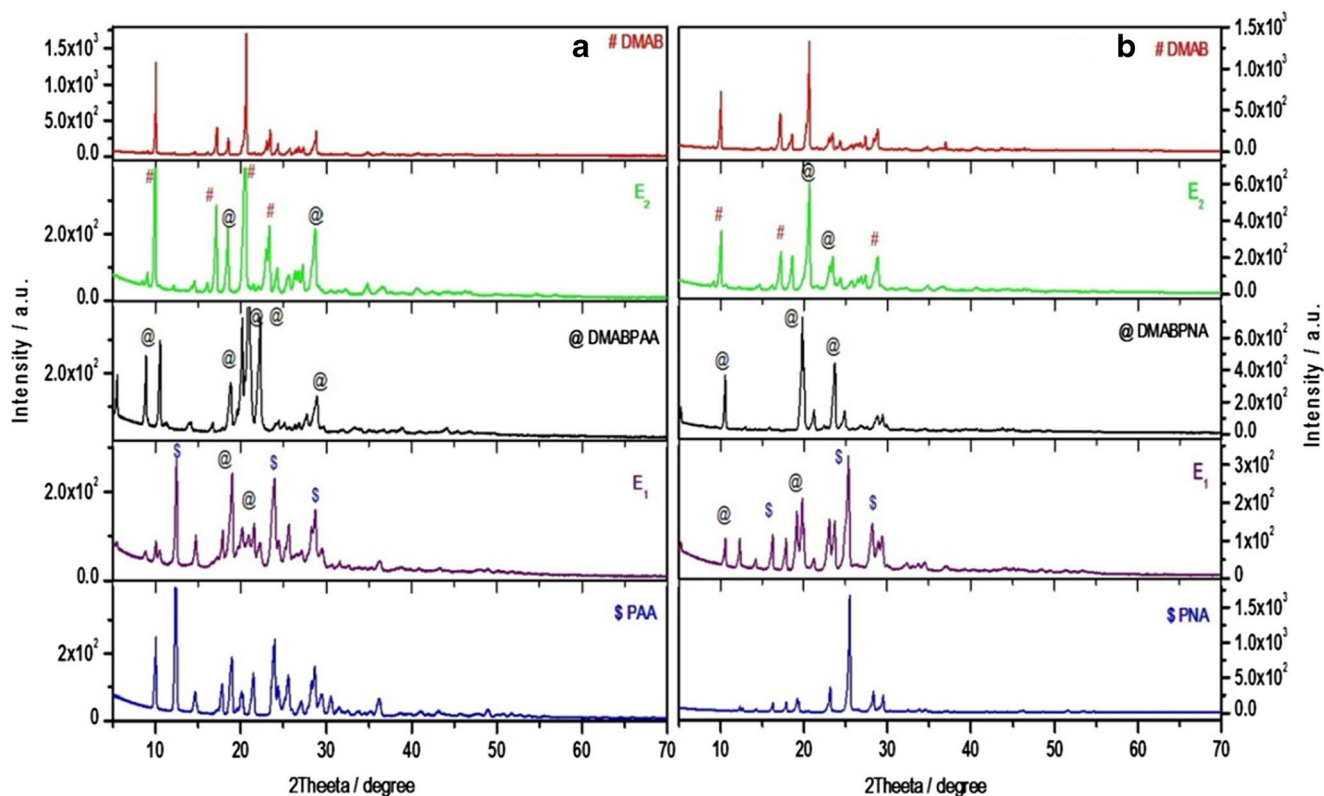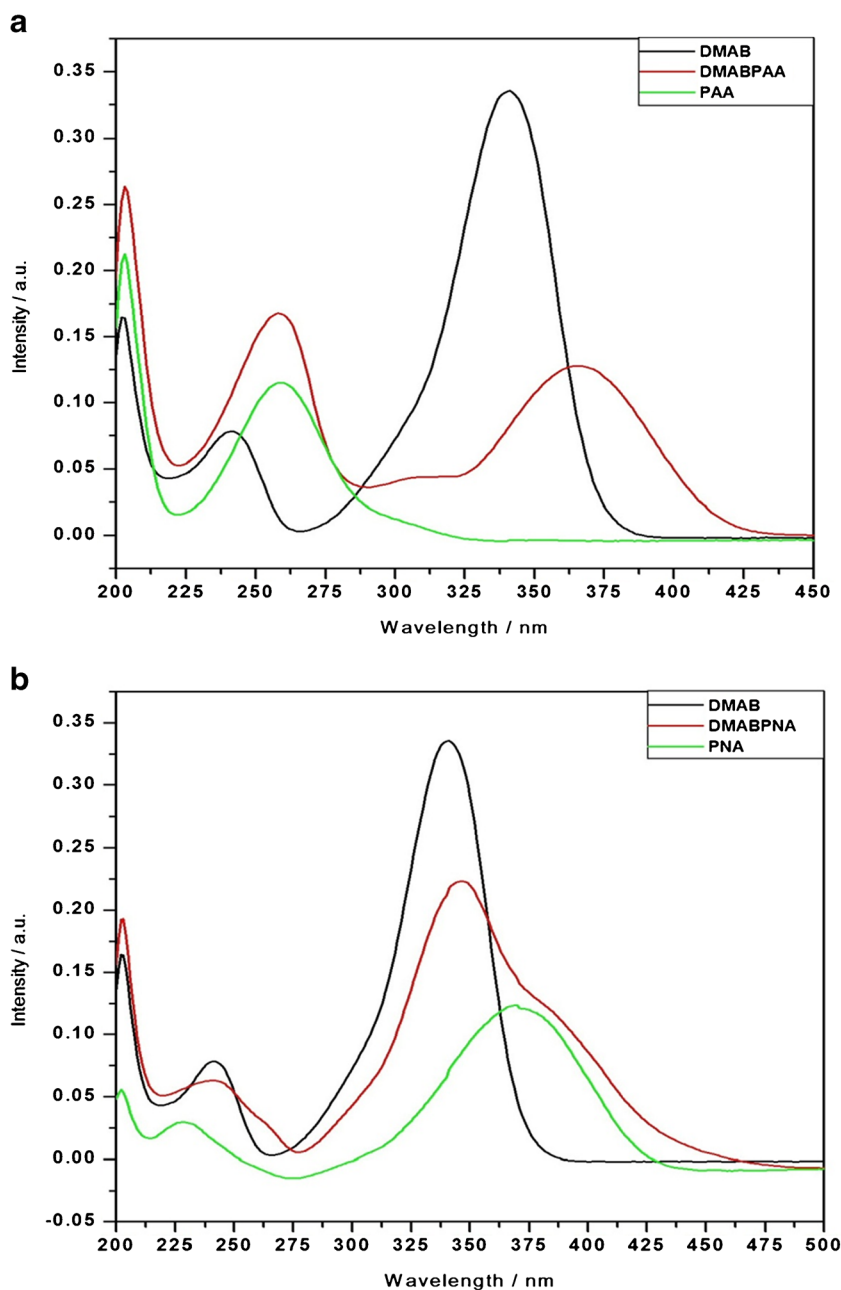

Fig. 6 Powder XRD of (**a**) DMABPAA, DMAB, PAA and eutectics (**b**) DMABPNA, DMAB, PNA and eutectics

strong fluorescence at 355 nm with Stoke's shift 97 nm for DMABPAA and stoke's shift of 104 nm for DMABPNA. The fluorescence quantum yield for both the novel complexes on excitation with their lower λ_{max} absorption band were calculated [42] using well known organic fluorescent pyrene (ϕ=0.75) material as reference. The same solvent (MeOH) was used for each samples and the concentration was maintained to be uniform (10^{-5} M) at room temperature and the quantum yield values thus obtained are tabulated in Table 4. These phenomena are attributed to the formation of a cyclic secondary amine moiety and due to excited state intra-molecular charge transfer (ICT) process [43]. The fluorescence spectra of both complex compounds, DMABPAA and DMABPNA, along with their respective parent compounds are shown in Fig. 8b, c, respectively. For comparison the fluorescence spectra of complexes along with reference pyrene materials are shown in Fig. 8d.

Conclusion

The phase diagram study of 4-dimethylaminobenzaldehyde (DMAB)–4-aminoacetanilide (PAA) and DMAB–4-nitroaniline (PNA) show the formation of novel organic complex compounds, DMABPAA and DMABPNA, in 1:1 molar ratio. The complexes have shown their congruent melting
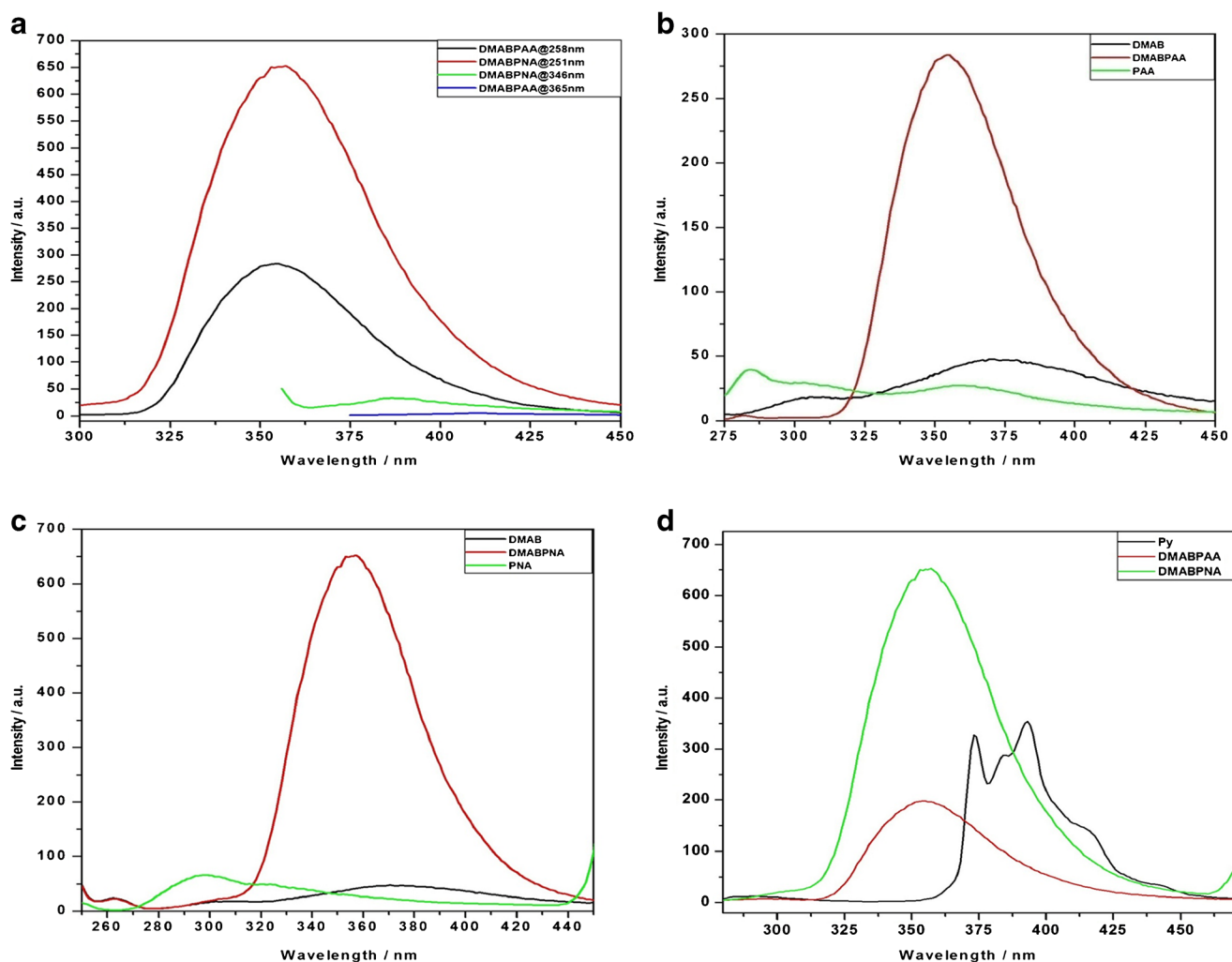
Fig. 8 a) Fluorescence spectra of DMABPAA and DMABPNA complexes at different excitation. **b**) Fluorescence spectra of DMABPAA, DMAB and PAA at λ_{ex}. 258 nm. **c**) Fluorescence spectra of DMA-BPNA, DMAB and PNA at λ_{ex}. 251 nm **d**) Fluorescence spectra of DMABPAA, DMABPNA and pyrene

nature at 218 °C for DMABPAA and 202 °C for DMA-BPNA. The single, sharp and higher melting temperature than parents compounds obtained from DSC curve for both complex compounds infers the stability and novelty of the newly synthesized materials. The studied various thermodynamics parameters like heat of fusion, entropy of fusion,

Table 4 UV–vis absorption, fluorescence, stoke's shift and quantum yield of complexes

Compound	Solvent	Absorption λ (nm)	Fluorescence λ (nm)	Stoke's shift $\Delta\nu$ (cm^{-1})	Quantum Yield (φ)
DMAB-PAA	Methanol	258	355	10,590	0.66
DMA-BPNA	Methanol	251	355	11,671	0.93

heat of mixing, excess thermodynamic functions, interfacial energy, roughness parameter and Grain boundary energy of the novel complexes as well as their binary eutectics infers the thermo chemical behaviour of synthesized materials. The FTIR and NMR spectroscopic studies of complexes support the findings of phase diagram and formation of new entities. It also concludes the covalent nature of interaction between the parent moieties to yield the complexes. The appearance of some new and intense peaks in the powder XRD studies of complexes further confirmed the novelty and crystanallity of the complexes. The absorption spectra of the complexes at lower absorption band show bathochromic shift with increased intensity due to increase in extent of conjugation. The fluorescence emission spectra of the complexes were found significantly higher with higher fluorescence quantum yield 0.66 (DMABPAA) and 0.93 (DMABPNA) compared to their parent compounds. These novel compounds

are having compatible fluorescence emission to that of well known pyrene organic material, which infers the future applicability of the synthesized materials.

References

1. Smart LE, Moore EA (2012) Solid state chemistry: an introduction. CRC Press
2. Singh NB, Dwivedi KD (1982) Chemistry and solidification behavior of eutectics. J Sci Ind Res 41:98–116
3. Gupta RK, Singh RA (2004) Thermochemical and microstructural studies on binary organic eutectics and complexes. J Cryst Growth 267(1):340–347
4. Kim SG et al (2004) Phase-field modeling of eutectic solidification. J Cryst Growth 261(1):135–158
5. Witusiewicz VT et al (2006) Phase equilibria and eutectic growth in ternary organic system (D) camphor–neopentylglycol–succinonitrile. J Cryst Growth 286(2):431–439
6. Singh NB, Giri DP, Singh NP (1999) Solid – liquid equilibria for p-dichlorobenzene + p-dibromobenzene and p-dibromobenzene + resorcinol. J Chem Eng Data 44(3):605–607
7. Suk M-J, Leonartz K (2000) Halo growth during unidirectional solidification of camphor–naphthalene eutectic system. J Cryst Growth 213(1):141–149
8. Rastogi RP et al (1981) Chemistry of binary and ternary organic eutectics. Mol Cryst Liq Cryst 73(1-2):7–34
9. Pigon K, Krajewska A (1983) Phase diagrams in the binary systems of 2,4,7-trinitrofluoren-9-one with aromatic and heteroaromatic compounds II thermodynamic analysis, chemischer informationsdienst 14.3
10. Togashi A, Matsunga Y (1987) Bull Chem Soc Jpn 69(B):1171
11. Bassi PS, Sharma NK, Sharma MK (1983) Mode of solidification and strength properties (II) naphthalene-benzil binary system. Cryst Res Technol 18(9):1191–1197
12. Shaanan M, Kalish R, Richter V (1986) Measurement of Be-profiles by the 9Be (p, α) 6Li reaction. Nucl Instrum Methods Phys Res Sect B: Beam Interact Mater Atoms 16(1):56–60
13. Sifaoui H, Rogalski M (2012) Solid–liquid equilibria of three binary systems of anthracene with 2-phenylimidazole, 4, 5-diphenylimidazole and 2, 4, 5-triphenylimidazole. Thermochim Acta 543:32–36
14. Rai US, George S (1994) Thermochemical studies on the eutectics and addition compounds in the binary systems of benzidine with p-nitrophenol, m-aminophenol and resorcinol. Thermochim Acta 243(1):17–25
15. Soos ZG (1974) Theory of π-molecular charge-transfer crystals. Annu Rev Phys Chem 25(1):121–153
16. Wasielewski MR (1992) Photoinduced electron transfer in supramolecular systems for artificial photosynthesis. Chem Rev 92(3):435–461
17. Nandi N, Bhattacharyya K, Bagchi B (2000) Dielectric relaxation and solvation dynamics of water in complex chemical and biological systems. Chem Rev 100(6):2013–2046
18. Chemla DS, Zyss J (1987) Nonlinear optical properties of organic molecules and crystals academic. New York p19872
19. Maeda M (1984) Laser Dyes Academic Press, New York
20. Kalyanasundaram K (2012) Photochemistry in microheterogeneous systems. Elsevier
21. Saroja G et al (1999) The fluorescence response of a structurally modified 4-aminophthalimide derivative covalently attached to a fatty acid in homogeneous and micellar environments. J Phys Chem B 103(15):2906–2911
22. Korolkovas A (1998) Essentials of medicinal chemistry, 2nd edn. Wiley, New York Ch. 3
23. Mandal R, Lahiri SC (1999) Interactions of L-amino acids with metronidazole and tinidazole. J Indian Chem Soc 76(7):347–349
24. Gao B, Zhu J-L (2008) 4-(Dimethylamino)benzaldehyde. Acta Crystallogr Sect E: Struct Rep Online 64(7):1182–1182
25. Khalil OS, Seliskar CJ, McGlynn SP (1973) Electronic spectroscopy of highly-polar aromatics II luminescence of nitroanilines. J Chem Phys 58(4):1607–1612
26. Karna SP, Paras N, Prasad DM (1991) Nonlinear optical properties of p-nitroaniline: an ab initio time-dependent coupled perturbed Hartree–Fock study. J Chem Phys 94(2):1171–1181
27. Isaeva GA, Isaev PP (1992) Quantum-chemical analysis of anesthetics effect on excitable biomembranes. Zh Fiz Khim 66(4):999–1006
28. Scott A (1992) Davydov's soliton. Phys Rep 217(1):1–67
29. Haisa M et al (1977) The crystal and molecular structures of p-aminoacetanilide and p-methylacetanilide. Acta Crystallogr Sect B: Struct Crystallogr Cryst Chem 33(8):2449–2454
30. Bouchouit K et al (2008) Structural phase transition and nonlinear optical properties in p-nitroaniline, Mediterranean winter. ICTON MW 2008
31. Dean JA (1985) Lange's handbook of chemistry. McGraw-Hill, New York
32. Reddi RSB et al (2009) Crystallization, thermal, phase diagram and microstructural studies of organic analog of metal–nonmetal monotectic alloy: 4-Bromochlorobenzene–succinonitrile. J Cryst Growth 312(1):95–99
33. Singh N et al (1985) Thermochim Acta 95(1):291–293
34. Singh M et al (2013) Solid–liquid equilibrium, thermal, and physicochemical studies on salicylamide–4-nitrophenol and 2-cyanoacetamide–4-aminoacetophenone organic eutectic systems. J Therm Anal Calorim 113(2):977–983
35. Reddi RSB, Kumar Satuluri VSA, Rai RN (2011) Solid–liquid equilibrium, thermal and physicochemical studies of organic eutectics. J Therm Anal Calorim 107(1):183–188
36. Kemp W (1993) Organic spectroscopy, 3rd edition, ELBS, Macmillan
37. Singh M et al (2015) Synthesis, crystal growth and physicochemical studies on a novel organic inter-molecular compound; 3,5-dinitrobenzoic acid and salicylamide system. J Cryst Growth 419:114–122
38. Kalsi PS (2005) Spectroscopy of organic compounds, Sixth edn. New Age Publication, India, pp 1–12
39. Koppel IA et al (1994) The gas-phase acidities of very strong neutral Bronsted acids. J Am Chem Soc 116(7):3047–3057
40. Koppel IA et al (2001) The enormous acidifying effect of the supersubstituent NSO 2 CF 3 on the acidity of derivatives of benzenesulfonamide and toluene-p-sulfonamide in the gas phase and in dimethyl sulfoxide. J Chem Soc Perkin Trans 2(2):229–232
41. Yuvaraj AR et al (2016) Photo-inhibition effect from strong electron withdrawing nitro group in N-[(E)-(4-bromophenyl) methylidene]-4-nitroaniline. Chem Adv Mater 1(1):1–5
42. Karpovich DS, Blanchard GJ (1995) Relating the polarity-dependent fluorescence response of qrene to vibronic coupling, achieving a fundamental understanding of the py polarity scale. J Phys Chem 99:3951–3958
43. Bani-Yaseen AD, Hammad F, Ghanem BS, Mohammad EG (2013) J Fluoresc 23:93–101